Semiempirical specification of singlet-triplet mixing angles, oscillator strengths, and g factors in $nsn'l$, $nsn'p^5$, np^2, and np^4 configurations

Lorenzo J. Curtis
Department of Physics and Astronomy, University of Toledo, Toledo, Ohio 43606
(Received 24 July 1989)

Methods are presented for determining singlet-triplet mixing angles from measured energy-level data in two-valence electron systems, and for utilizing these mixing angles to specify $E1$ and $M1$ oscillator strengths and magnetic g factors from LS coupling and hydrogenic formulas and from data obtained in single-valence electron systems. These methods are tested through studies of line strengths in the He, Mg, Ne, Si, and S isoelectronic sequences and of g factors in the Kr and Pb atoms.

I. INTRODUCTION

Measurements of atomic energy levels, oscillator strengths, and magnetic g factors provide three complementary types of information that bear on the specification of the wave function of the system. Energy-level data are usually of much higher precision (typically parts in 10^8) than oscillator strength or g-factor data (typically parts in 10^2) and systematic trends in energy-level data also often permit accurate interpolations and extrapolations along isoelectronic sequences.[1] These three types of information can be deduced directly from *ab initio* theory, but it is sometimes possible to utilize measured energy-level data to obtain more reliable semiempirical estimates of oscillator strengths[2] and of g factors.

Oscillator strengths for single-valence electron systems are often accurately predicted by methods that incorporate measured energy-level data into the calculation. Semiempirical predictions can be obtained by various quasihydrogenlike approaches[3] such as the Coulomb approximation, the quantum-defect method, and model potential calculations. In their simplest implementation these approaches employ a single-configuration computation of the $E1$ transition moment, but configuration interaction, core polarization, and other electron correlation, etc., are partially included through the use of experimental energy-level data. As will be shown below, results obtained for single-valence electron systems can sometimes be applied to two-valence electron systems through semiempirical specification of the effects of intermediate coupling. For magnetic properties such as $M1$ transition probabilities and magnetic moment g factors, the specification of intermediate coupling effects is even more direct.

For systems with two out-of-shell electrons, singlet-triplet, and L-state mixing within a given configuration manifests itself in the energy splittings, oscillator strengths, and g factors of the constituent levels. In intermediate coupling, the wave functions of levels with common J become a mixture of LS basis states that are not subject to the ΔL and ΔS selection rules that restrict their constituent amplitudes. The degree of intermediate coupling usually increases with increasing ionicity along an isoelectronic sequence (although counter examples exist, cf. Sec. III A). In fully *ab initio* calculations, intermediate coupling is implicitly included in the construction of the wave function. It is also possible[4] to empirically determine the mixing amplitudes explicitly from energy-level data, to combine these with semiempirical methods normally applied to single-electron systems, and thereby to semiempirically specify oscillator strengths and g factors for two-electron systems in intermediate coupling.

The purpose here is to generalize earlier calculations of this type for $nsn'l$ configurations[4] and to extend their use to $nsn'p^5$, np^2 and np^4 configurations. Although these four types of configurations may seem restrictive, they occur as either the ground or the first excited configuration in over one-fourth of the isoelectronic sequences of the stable elements. The ground configurations include ns^2np^2 for the C, Si, Ge, Sn, and Pb sequences; and ns^2np^4 for the O, S, Se, Te, and Po sequences. The first excited configurations include $nsnp$ for the Be, Mg, Zn, Cd, and Hg sequences; $(n-1)dns$ for the Ca, Sr, Ba, and Ra sequences (which becomes the ground configuration above some ionization stage in the sequence); and $(n-1)p^5ns$ for the Ne, Ar, Kr, Xe, and Rn sequences.

Formulas are presented below which specify singlet-triplet mixing angles in terms of energy-level data, and apply them, together with single-particle $E1$ line strengths and LS values for $M1$ line strengths and Landé g factors, to the prediction of two-particle line strengths and g factors. Tests of these procedures are presented for line strengths in the He, Mg, Ne, Si, and S isoelectronic sequences and for g factors in the Kr and Pb atoms.

II. CALCULATION OF MIXING ANGLES FROM ENERGY-LEVEL DATA

The $nsn'l$, $nsn'p^5$, np^2, and np^4 configurations were selected for study here because they contain no more than two levels of the same J, so that intermediate coupling connects the LS basis states only pairwise. Concise specification can thus be made in terms of two-by-two off-diagonal matrices, for which diagonalization can be

achieved by solution of quadratic (rather than cubic or higher-degree) equations. A matrix of the form

$$\underline{M}=\begin{bmatrix} a & c \\ c & b \end{bmatrix} \tag{1}$$

can be diagonalized by a basis transformation $\underline{T}^{-1}\underline{M}\,\underline{T}$, where

$$\underline{T}=\begin{bmatrix} \cos(\theta_J) & \sin(\theta_J) \\ -\sin(\theta_J) & \cos(\theta_J) \end{bmatrix} . \tag{2}$$

Here θ_J is the mixing angle, given by

$$\sin(\theta_J)=\{1+[W_J\pm(1+W_J^2)^{1/2}]^2\}^{-1/2} , \tag{3}$$

where

$$W_J\equiv(b-a)/2c . \tag{4}$$

In the cases to be considered, the quantities a, b, and c can be determined from experimental energy-level data and used to evaluate θ_J. The sign ambiguity in Eq. (3) is resolved by requiring that $\theta_J=0$ in the LS limit. This formulation specifies the mixing coefficients of the wave function for each pair of states with angular momentum J.

A. Mixing angles for $nsn'l$ and $nsn'p^5$ configurations

The $nsn'l$ configuration consists of four levels which, in the limit of pure LS coupling, can be denoted by $^3L_{l-1}$, ^3L_l, $^3L_{l+1}$, and ^1L_l. In intermediate coupling these levels can be specified in terms of the exchange Slater energy G_l, the spin-orbit energy ζ_l, and a common energy F_0 that includes the electron-nucleus energies, the electron-electron direct Slater energies, and (for excitation energies) the ionization potential. The Hamiltonian matrix elements[5] for this configuration in the LS representation are given in Table I. The $nsn'p^5$ configuration is described by the same matrix with the value $l=1$ and the substitution $\zeta_l\Longrightarrow-\zeta_l$.

The $J=l$ submatrix to be diagonalized is of the form of Eq. (1) with

$$\begin{aligned} a&=F_0-G_l-\zeta_l/2 , \\ b&=F_0+G_l , \\ c&=\sqrt{l(l+1)}\,\zeta_l/2 . \end{aligned} \tag{5}$$

With these values, Eqs. (4) and (5) yield, for the $J=l$ levels,

$$W_l=(4G_l+\zeta_l)/2\sqrt{l(l+1)}\,\zeta_l . \tag{6}$$

Although the diagonalized energies involve square roots and squares, the centroid of the energy for each J value is linear in the Slater parameters. Denoting the new composite states by primes, the J-centroid energies ε_J are given by

$$\begin{aligned} \varepsilon_{l-1}&=E(^3L_{l-1})=F_0-G_l-(l+1)\zeta_l/2 , \\ \varepsilon_l&=[E(^3L_l')+E(^1L_l')]/2=F_0-\zeta_l/4 , \\ \varepsilon_{l+1}&=E(^3L_{l+1})=F_0-G_l+l\zeta_l/2 , \end{aligned} \tag{7}$$

which can be solved simultaneously to obtain

$$\begin{aligned} \zeta_l&=2(\varepsilon_{l+1}-\varepsilon_{l-1})/(2l+1) , \\ G_l&=(2\varepsilon_l-\varepsilon_{l+1}-\varepsilon_{l-1})/2 . \end{aligned} \tag{8}$$

The mixing angle θ_l can be specified directly in terms of the physical energies by use of Eqs. (6) and (8), yielding

$$W_l=-\frac{l\varepsilon_{l+1}-(2l+1)\varepsilon_l+(l+1)\varepsilon_{l-1}}{\sqrt{l(l+1)}(\varepsilon_{l+1}-\varepsilon_{l-1})} . \tag{9}$$

Equation (9) can be substituted into Eq. (3) to specify the mixing angle θ_J in terms of the measured J-centroid energies. In terms of the LS basis states, the wave functions for the physical states are therefore

$$\begin{aligned} |^3L_{l-1}'\rangle&=|^3L_{l-1}\rangle , \\ |^3L_l'\rangle&=\cos(\theta_l)|^3L_l\rangle-\sin(\theta_l)|^1L_l\rangle , \\ |^3L_{l+1}'\rangle&=|^3L_{l+1}\rangle , \\ |^1L_l'\rangle&=\sin(\theta_l)|^3L_l\rangle+\cos(\theta_l)|^1L_l\rangle . \end{aligned} \tag{10}$$

The 1s2p and 1s3d terms in the He isoelectronic sequence

The validity of this approach is demonstrated in Fig. 1 for the case of the $1s2p$ and $1s3d$ terms in the helium isoelectronic sequence. For these systems highly accurate theoretical values for the energy levels,[6,7] mixing angles,[8–11] and transition probabilities[12] are available, permitting stringent tests of this formalism. The solid lines in Fig. 1 represent values for the mixing angle obtained by substitution of published energy-level data[6,7] into Eqs. (3) and (9), whereas the symbols denote *ab initio* values for the mixing angle computed directly from the wave

TABLE I. Hamiltonian matrix in the LS representation $\langle {}^sL_J|\mathcal{H}|{}^{s'}L_{J'}\rangle$ for the configurations $nsn'l$ and (with $l\Longrightarrow1$ and $\zeta_l\Longrightarrow-\zeta_l$)$nsn'p^5$.

	$^3L_{l-1}$	^3L_l	$^3L_{l+1}$	^1L_l
$^3L_{l-1}$	$F_0-G_l-(l+1)\zeta_l/2$	0	0	0
^3L_l	0	$F_0-G_l-\zeta_l/2$	0	$\sqrt{l(l+1)}\,\zeta_l/2$
$^3L_{l+1}$	0	0	$F_0-G_l+l\zeta_l/2$	0
^1L_l	0	$\sqrt{l(l+1)}\,\zeta_l/2$	0	F_0+G_l

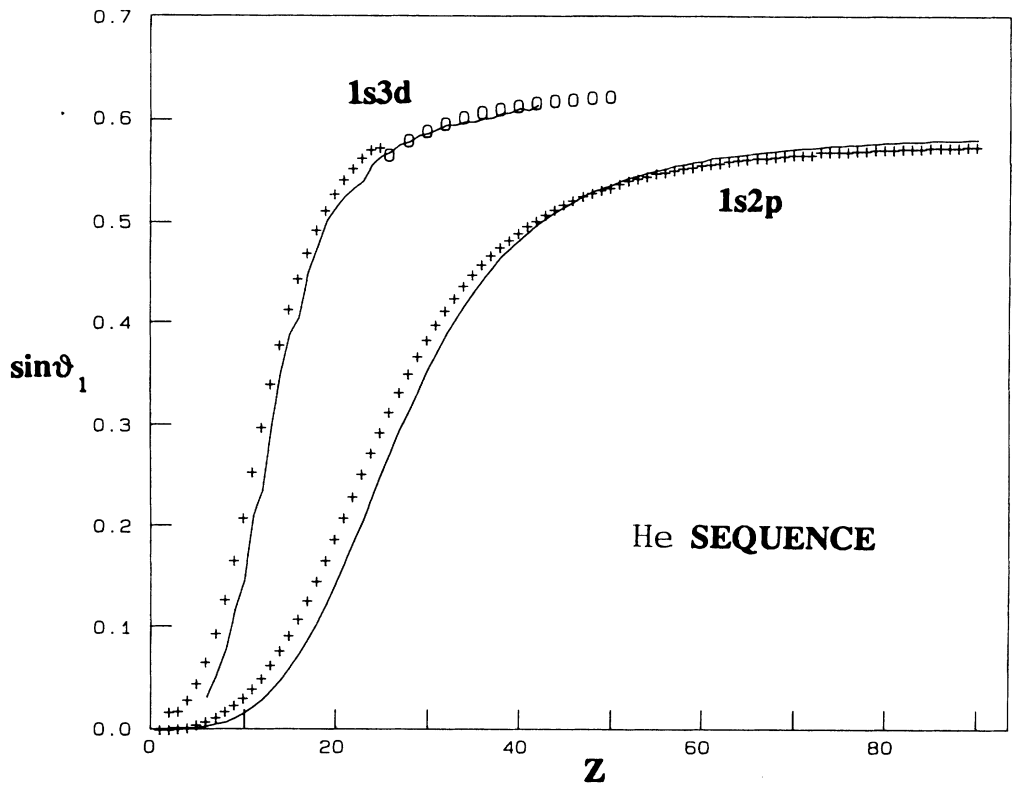

FIG. 1. Singlet-triplet mixing angles for the $1s2p\ ^{1,3}P$ and $1s3d\ ^{1,3}D$ levels in the He isoelectronic sequence. Solid curves represent values obtained by diagonalization of the matrix of energy levels (Refs. 8 and 9) and symbols represent direct *ab initio* calculations by Drake (Refs. 8 and 9) (+) and by Ermolaev and Jones (Ref. 10) (○).

functions by Drake[8,9] (+) and by Ermolaev and Jones[10] (○). It is clear from Fig. 1 that, despite its single configuration basis, this formulation specifies the Z variation of the mixing angle very accurately. If the empirical values are shifted downward by one stage of ionization, then the curves are virtually coincident.

B. Mixing angles for np^2 and np^4 configurations

The np^2 and np^4 configurations contain five levels which, in pure LS coupling, can be denoted as $^3P_{0,1,2}$, $^1D_2$, and $^1S_0$. These systems occur both in ground-state configurations of the form ns^2np^2 and ns^2np^4, and in multiply excited configurations. In addition to the F_0 and ζ_l quantities described above, the energies of these equivalent electrons also depend on the direct electron-electron Slater energy F_2. The Hamiltonian matrix elements[5] for the np^2 configuration in the LS representation are given in Table II, and the corresponding values for the np^4 configuration are obtained by the replacement $\zeta_p \Longrightarrow -\zeta_p$.

In these cases there are two matrix diagonalizations to be performed. First, there is $^1S_0$ and $^3P_0$ mixing, for which the submatrix of Eq. (1) involves

$$\begin{aligned} a &= F_0 - 5F_2 - \zeta_p \ , \\ b &= F_0 + 10F_2 \ , \\ c &= -\sqrt{2}\zeta_p \ , \end{aligned} \tag{11}$$

so that, for the $J=0$ levels, Eqs. (4) and (11) yield

$$W_0 = -(15F_2 + \zeta_p)/2\sqrt{2}\zeta_p \ . \tag{12}$$

Second, there is $^1D_2$-$^3P_2$ mixing, for which the submatrix of Eq. (1) involves

TABLE II. Hamiltonian matrix in the LS representation $\langle {}^sL_J|\mathcal{H}|{}^{s'}L_{J'}\rangle$ for the configurations np^2 and (with the substitution $\zeta_p \Longrightarrow -\zeta_p$) np^4.

	$^3P_0$	$^3P_1$	$^3P_2$	$^1D_2$	$^1S_0$
$^3P_0$	$F_0-5F_2-\zeta_p$	0	0	0	$-\sqrt{2}\zeta_p$
$^3P_1$	0	$F_0-5F_2-\zeta_p/2$	0	0	0
$^3P_2$	0	0	$F_0-5F_2+\zeta_p/2$	$\zeta_p/\sqrt{2}$	0
$^1D_2$	0	0	$\zeta_p/\sqrt{2}$	F_0+F_2	0
$^1S_0$	$-\sqrt{2}\zeta_p$	0	0	0	F_0+10F_2

$$a=F_0-5F_2+\zeta_l/2\ ,$$
$$b=F_0+F_2\ , \tag{13}$$
$$c=\zeta_p/\sqrt{2}\ ,$$

so that for the $J=2$ levels, Eqs. (4) and (13) yield

$$W_2=(12F_2-\zeta_p)/2\sqrt{2}\zeta_p\ . \tag{14}$$

In this case the J-centroid energy values are

$$\varepsilon_0=[E(^1S_0')+E(^3P_0')]/2=F_0+5F_2/2-\zeta_p/2\ ,$$
$$\varepsilon_1=E(^3P_1)=F_0-5F_2-\zeta_p/2\ , \tag{15}$$
$$\varepsilon_2=[E(^1D_2')+E(^3P_2')]/2=F_0-2F_2+\zeta_p/4\ ,$$

which can be solved simultaneously to obtain

$$\zeta_p=4(5\varepsilon_2-2\varepsilon_0-3\varepsilon_1)/15\ ,$$
$$F_2=2(\varepsilon_0-\varepsilon_1)/15\ . \tag{16}$$

Equations (12) and (14) can be expressed in terms of measured energies using Eqs. (16) to obtain

$$W_0=-\frac{10\varepsilon_2-21\varepsilon_1+11\varepsilon_0}{4\sqrt{2}(5\varepsilon_2-3\varepsilon_1-2\varepsilon_0)} \tag{17}$$

and

$$W_2=-\frac{5\varepsilon_2+3\varepsilon_1-8\varepsilon_0}{2\sqrt{2}(5\varepsilon_2-3\varepsilon_1-2\varepsilon_0)}\ . \tag{18}$$

Substitution of Eqs. (17) and (18) into Eq. (3) permits the mixing angles to be specified in terms of the measured J-centroid energies. In terms of the LS basis states, the wave functions for the physical states are therefore

$$|^3P_0'\rangle=\cos(\theta_0)|^3P_0\rangle-\sin(\theta_0)|^1S_0\rangle\ ,$$
$$|^3P_1'\rangle=|^3P_1\rangle\ ,$$
$$|^3P_2'\rangle=\cos(\theta_2)|^3P_2\rangle-\sin(\theta_2)|^1D_2\rangle\ , \tag{19}$$
$$|^1D_2'\rangle=\sin(\theta_2)|^3P_2\rangle+\cos(\theta_2)|^1D_2\rangle\ ,$$
$$|^1S_0'\rangle=\sin(\theta_0)|^3P_0\rangle+\cos(\theta_0)|^1S_0\rangle\ .$$

III. TRANSITION PROBABILITIES, OSCILLATOR STRENGTHS, AND LINE STRENGTHS

In terms of the line strengths, the transition rates A for the $E1$ transitions are given by[13]

$$(2J_k+1)A_{E1}(k,i)=(2.0261\times10^{-6}\ \text{cm}^3/\text{s})\times[E(k)-E(i)]^3S_{E1}(i,k)\ , \tag{20}$$

where

$$S_{E1}=|\langle i\|\mathbf{r}\|k\rangle|^2\ . \tag{21}$$

Here $\mathbf{r}$ is in units of a_0, and S_{E1} scales isoelectronically as $1/Z^2$. For $M1$ transition rates[13]

$$(2J_k+1)A_{M1}(k,i)=(2.6973\times10^{-11}\ \text{cm}^3/\text{s})\times[E(k)-E(i)]^3S_{M1}(i,k)\ , \tag{22}$$

where

$$S_{M1}=|\langle i\|\mathbf{L}+g_e\mathbf{S}\|k\rangle|^2\ . \tag{23}$$

Here g_e is the g factor of the electron, $\mathbf{L}$ and $\mathbf{S}$ are in units of $\hbar$, and S_{M1} scales isoelectronically as independent of Z. In either case, the absorption oscillator strength f is given by[13]

$$(2J_i+1)f(i,k)=(1.4992\ \text{s/cm}^2)\times[E(k)-E(i)]^{-2}(2J_k+1)A(k,i)\ . \tag{24}$$

If either the bra or the ket in Eqs. (21) or (23) involves composite LS basis states as in Eqs. (10) and (19), then the line strengths will consist of mixing angle factors and LS values for the line strengths. Various methods for the evaluation of S_{E1} will be discussed in subsections below.

For magnetic dipole transitions, the line strength factors S_{M1} for pure LS coupling connect only states that differ at most by the J quantum number, and depend only on angular factors, involving simple rational fractions given by[14,15]

$$S_{M1}(LSJ,LSJ\pm1)=(+1)^2[(L+S+1)^2-J_>^2]\times[J_>^2-(L-S)^2]/4J_>\ ,$$
$$S_{M1}(LSJ,LSJ)=(+1)^2(2J+1)\times[S(S+1)-L(L+1)+3J(J+1)]^2/4J(J+1)]\ , \tag{25}$$

where the factor $(+1)^2$ denotes the sign of the unsquared quantity in Eq. (23).

Since the considerations made here assume that precise energy-level data are available, the transition probabilities and oscillator strengths can be uniquely specified in terms of the line strengths and energy separations. Thus (avoiding ambiguities in the use of experimental or theoretical energy levels to convert among theoretical line strengths, oscillator strengths, and transition probabilities) presentations in the subsections below will compare isoelectronically scaled line strengths: Z^2S_{E1} for the $E1$ case; S_{M1} for the $M1$ case.

A. Line strengths for $nsn'l$ and $nsn'p^5$ configurations

For an $nsn'p$ configuration, the most common type of $E1$ transition connects it to a nearby $ns^2\,^1S_0$ state. Similarly, for an $nsn'p^5$ configuration, the most common type of transition is to a nearby $n'p^6\,^1S_0$ state. These transitions can be specified in terms of the mixing amplitude of the $^1P_1$ LS state. The presence of the spectator ns or $n'p$ electrons is taken into account by the mixing angle, and these transitions can be specified using single-electron radial transition elements using

$$S_{E1}(^1S_0,^1P_1')=k\cos^2(\theta_1)|\langle ns|r|n'p\rangle|^2\ ,$$
$$S_{E1}(^1S_0,^3P_1')=k\sin^2(\theta_1)|\langle ns|r|n'p\rangle|^2\ , \tag{26}$$

where the factor k accounts for equivalent electrons and appropriate Racah algebra factors. The transition mo-

ment $\langle ns|r|n'p\rangle$ can be obtained by a number of semiempirical approaches, as will be discussed in the context of specific examples.

The $M1$ line strengths for these systems can be obtained using Eqs. (10) and (25), and are given by[4]

$$\begin{aligned} S_{M1}({}^3P_1', {}^3P_0) &= 2\cos^2(\theta_1) , \\ S_{M1}({}^3P_2, {}^3P_1') &= \tfrac{5}{2}\cos^2(\theta_1) , \\ S_{M1}({}^1P_1', {}^3P_0) &= 2\sin^2(\theta_1) , \\ S_{M1}({}^1P_1', {}^3P_1') &= \tfrac{3}{2}\cos^2(\theta_1)\sin^2(\theta_1) , \\ S_{M1}({}^1P_1', {}^3P_2) &= \tfrac{5}{2}\sin^2(\theta_1) . \end{aligned} \tag{27}$$

The $1s^2$-$1s2p$ transitions in the He isoelectronic sequence

An application of this method to $E1$ transitions in the He sequence is shown in Fig. 2. In pure LS coupling the $1s^2\,{}^1S_0$-$1s2p\,{}^1P_1$ resonance transition is $E1$ allowed, but the $1s^2\,{}^1S_0$-$1s2p\,{}^3P_1$ intercombination is $E1$ forbidden. In intermediate coupling both are allowed, and as seen in Eq. (26), the resonance and intercombination transition elements are multipiled by factors $\cos^2(\theta_1)$ and $\sin^2(\theta_1)$, which were computed and displayed in Fig. 1. Figure 2 shows a comparison between mixing angle predictions with two different semiempirical estimates of the transition moment, and the *ab initio* relativistic random-phase approximation (RRPA) calculations of Lin, Johnson, and Dalgarno.[12] The symbols denote the RRPA calculations, the solid lines represent results using empirical mixing angles and a Coulomb approximation calculation[16] of the transition moment, and the dotted lines represent the same calculation made using a screened hydrogenic approximation of the transition moment suggested by Dalgarno and Parkinson[17]

$$|\langle 1s|r|2p\rangle|^2 = 2^{15}/3^9(Z+0.155)^2 . \tag{28}$$

These three calculations are in close agreement for the intercombination line, and for the resonance line the Coulomb approximation follows RRPA reasonably well, although deviations occur at very high Z.

Figure 2 indicates that the mixing angle is a dominant consideration in this calculation, since a crude estimate of the transition moment can yield reasonably good predictions. While semiempirical methods are intended for (and are usually more successful in describing) complex many-electron systems, this He-sequence example provides a test of these methods in a case for which the energy levels can be considered precisely known over the entire isoelectronic sequence.

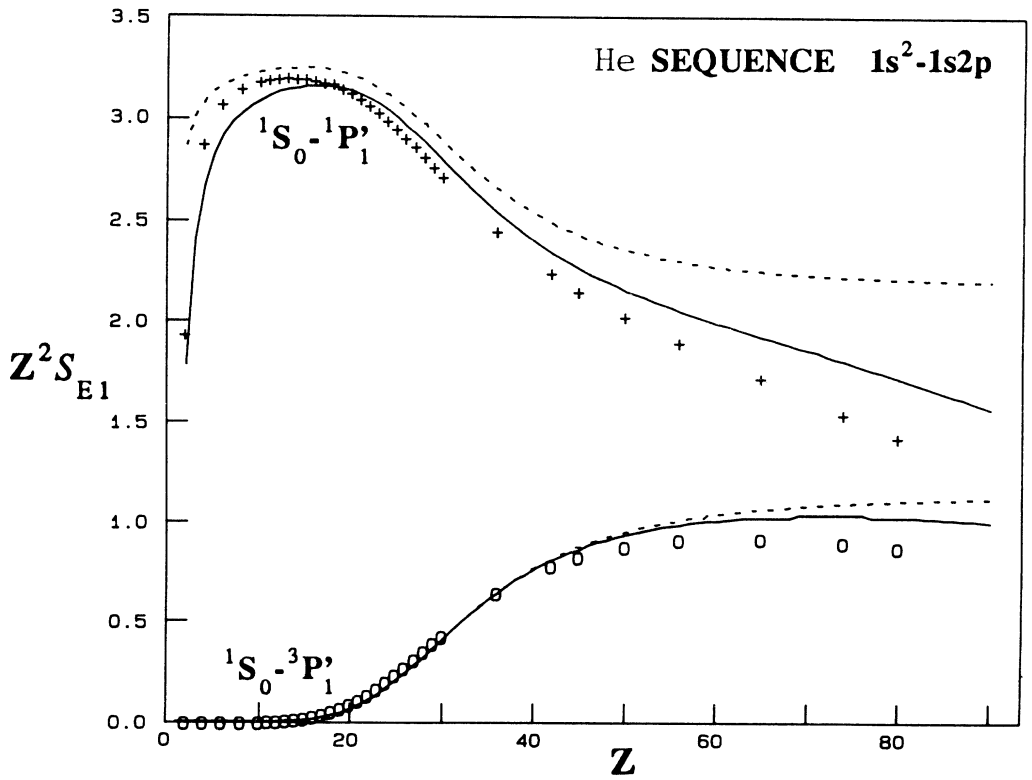

FIG. 2. Z-scaled line strengths for the $1s^2$-$1s2p$ transitions in the He isoelectronic sequence. Calculations using Eq. (26) with the semiempirical mixing angles from Fig. 1 are denoted by the solid curves (with the transition moment evaluated by the Coulomb approximation) and the dotted curves (with a screened hydrogenic value for the transition moment). The symbols represent *ab initio* RRPA calculations (Ref. 12) for the resonance (+) and intercombination (○) line strengths.

The $3s^2$-3s3p transitions in the Mg isoelectronic sequence

The ns^2-$nsnp$ resonance and intercombination transitions in alkalilike isoelectronic sequences are (in contrast to the He example above) unbranched, so their transition probabilities can be determined in level lifetime measurements. An application to the $n=3$ case of the Mg isoelectronic sequence is shown in Fig. 3. In this case, the values used for the single-particle $3s$-$3p$ transition moments were taken from the corresponding quantities in the Na isoelectronic sequence. Exclusive of the information contained in the mixing angles, the transition moments for these two sequences differ only through the presence of screening by an additional $3s$ spectator electron. It was found by least-squares-fitting methods that, by scaling squared transition moments for the Na isoelectronic sequence downward by a constant (Z-independent) multiplicative factor of 0.83, almost perfect agreement could be obtained with published *ab initio* line strengths in the Mg sequence.

The mixing angles are computed from experimental Mg sequence energy-level data[18] for $Z \leq 33$, which were supplemented by the theoretical values of Cheng and Johnson[19] for $36 \leq Z \leq 92$. The line strengths for the Na sequence were taken from the theoretical values of Kim and Cheng,[20] and the theoretical line strengths for the Mg sequence were taken from the calculations of Cheng and Johnson.[19] To retain the corresponding energy ordering of the two systems, the $J = \frac{1}{2}$-$\frac{1}{2}$ line strengths in the Na sequence were used to predict the intercombination line strengths in the Mg sequence, and the $J = \frac{1}{2}$-$\frac{3}{2}$ line strengths Na sequence were used to predict the resonance line strengths in the Mg sequence resonance lines (although the J dependence was slight).

As can be seen from Fig. 3, agreement between the semiempirical and *ab initio* values is excellent. While the multiplicative factor 0.83 is purely empirical, the fact that it is a single overall constant is important since it permits predictions of lifetimes based entirely on experimental data. If accurate energy-level data are available for both sequences and a data base for lifetimes in the Na sequence exists, then the multiplicative constant could be determined from a single accurate lifetime measurement (of either the singlet or triplet level) for one isolated ion in the Mg sequence. This permits lifetimes measured in the Na sequence to be used in the prediction of lifetimes in the Mg sequence using only singlet-triplet mixing angles determined from experimental energy-level data.

Qualitatively similar results were also obtained for the $n=2$ case, using energy-level and oscillator strength data for the Li and Be sequences from the multiconfiguration

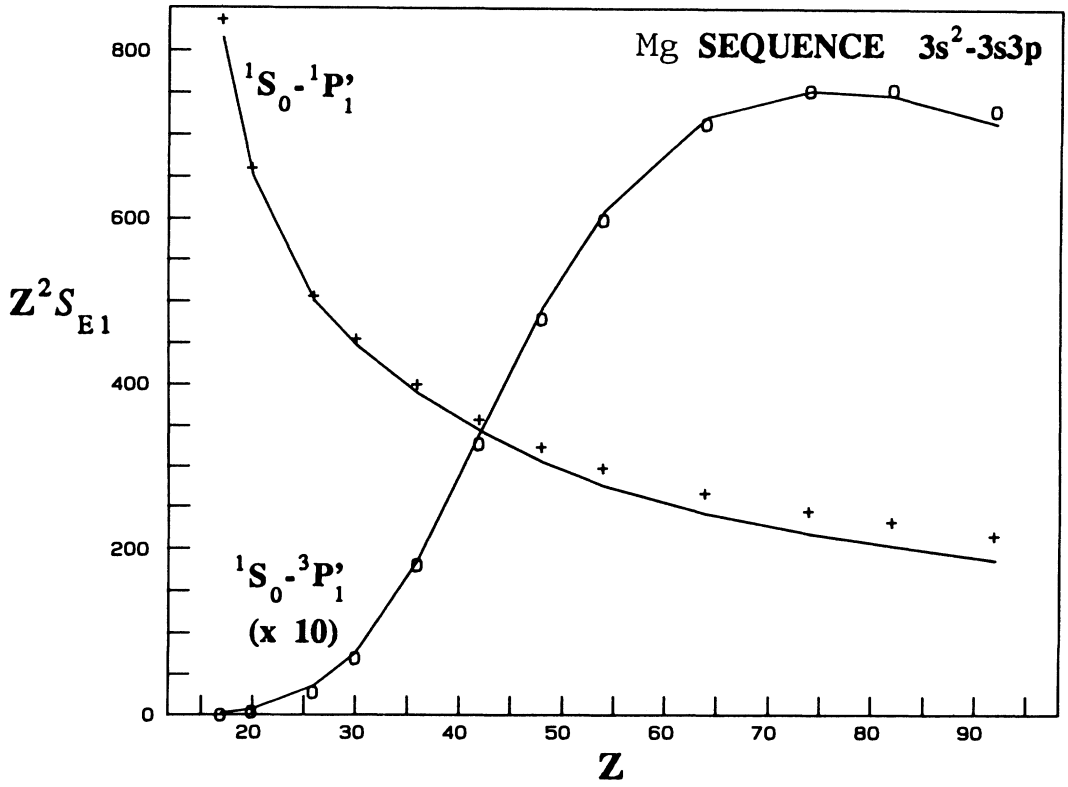

FIG. 3. Z-scaled line strengths for the $3s^2$-$3s3p$ transitions in the Mg isoelectronic sequence. The solid lines denote calculations using Eqs. (26) with empirical mixing angles, and the use of the transition moments for corresponding elements in the Na sequence, scaled downward by an empirical factor 0.83. The symbols represent *ab initio* calculations (Ref. 20) for the resonance (+) and intercombination (○) line strengths.

Dirac-Fock (MCDF) calculations Cheng, Kim, and Desclaux.[21] Mixing angles were obtained from the energy-level values for the Be sequence, and transition moments were obtained from the oscillator strength and energy values for the Li sequence. A scaling was again attempted by least-squares method, and it was found that by scaling the squared transition moment for the Li sequence downward by a constant (Z-independent) multiplicative factor of 0.70, the predictions of Eqs. (26) gave good agreement with the *ab initio* calculations[21] for the resonance and intercombination line strengths in the Be sequence. Application to both the Be (Li) and Mg (Na) sequences indicates that this technique also has homologous applicability.

The use of Eqs. (27) to accurately predict $M1$ transition probabilities in the Be, Mg, and Zn isoelectronic sequences was already demonstrated and compared with MCDF calculations in Ref. 4. Additional examples of the calculation of $M1$ line strengths will be given in Sec. III B.

The $2p^6$-$2p^5 3s$ transitions in the Ne isoelectronic sequence

Figure 4 presents an application to the $2p^6$-$2p^5 3s$ transitions in the Ne isoelectronic sequence. Here energy-level values for $20 \leq Z \leq 80$ were taken from the theoretical calculations of Ivanova and Glushkov[22] and used to compute the mixing angles. Line strengths were computed from Eqs. (26) using a simple fully screened hydrogenlike transition moment

$$|\langle 2p|r|3s\rangle|^2 = \text{const}/(Z-9)^2 . \tag{29}$$

For a true hydrogenlike ion, this constant would equal $2^{15}3^8/5^{12}=0.8806$. Good agreement with *ab initio* estimates was obtained (through least-squares methods) by adjusting this constant upward (by a factor of 2.20) to a value 1.94. The *ab initio* values for the line strength were deduced from calculations of oscillator strengths in the range $19 \leq Z \leq 34$ made by Biémont and Hansen.[23] As can be seen from Fig. 4, here again the agreement is excellent, especially in consideration of the complexity of the system and the simplicity of the model.

For these levels the spin mixing causes a crossover in the dominant configuration (i.e., $\theta_1=\pi/4$) at $Z \cong 18$, which has led to alternative labeling conventions in the literature. Furthermore, the isoelectronic behavior of this sequence is such that $\sin(\theta_1)$ first undergoes a retrograde *decrease* from Ne I to Na II before assuming the normal progression with Z from LS to jj coupling.[13] Consistent with the mixing angle formalism, the labels used in Fig. 4 are associated with the low-Z LS limit.

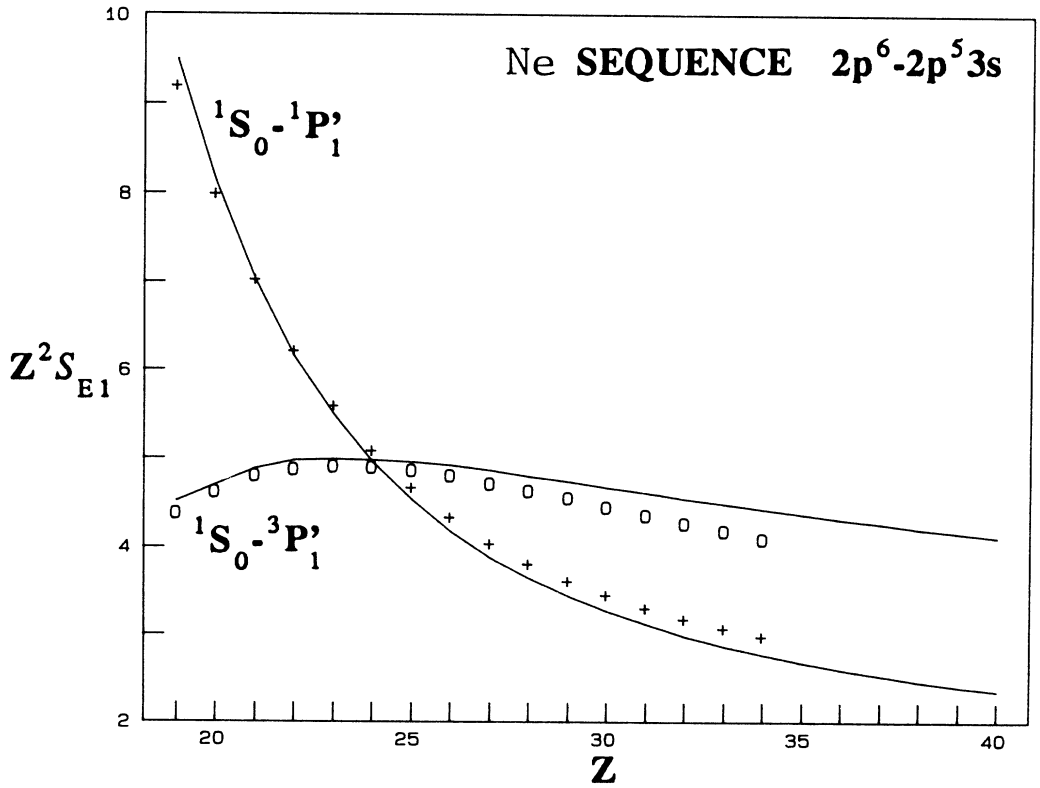

FIG. 4. Z-scaled line strengths for the $2p^6$-$2p^5 3s$ transitions in the Ne isoelectronic sequence. The solid lines denote calculations using Eqs. (26) with empirical mixing angles and a fully screened hydrogenlike transition moment, scaled upward by an empirical factor 2.20.

B. Line strengths for np^2 and np^4 configurations

Using Eqs. (19) and (23), the $M1$ line strengths for either an np^2 or np^4 configuration can be written as

$$
\begin{aligned}
&S_{M1}({}^3P_1,{}^3P_0')=2\cos^2(\theta_0)\ ,\\
&S_{M1}({}^3P_2',{}^3P_1)=\tfrac{5}{2}\cos^2(\theta_2)\ ,\\
&S_{M1}({}^1D_2',{}^3P_1)=\tfrac{5}{2}\sin^2(\theta_2)\ ,\\
&S_{M1}({}^1D_2',{}^3P_2')=\tfrac{15}{2}\cos^2(\theta_2)\sin^2(\theta_2)\ ,\\
&S_{M1}({}^1S_0',{}^3P_0')=0\ ,\\
&S_{M1}({}^1S_0',{}^3P_1)=2\sin^2(\theta_0)\ .
\end{aligned}
\tag{30}
$$

The $3s^23p^2$ and the $3s^23p^4$ configurations in the Si and S isoelectronic sequences

Figures 5 and 6 display the results of this approach applied to the calculation of line strengths for transitions within the ground configurations $3s^23p^2$ and $3s^23p^4$ of the Si and S isoelectronic sequences. The solid curves represent predictions [using Eqs. (30)] based on mixing angles deduced [using Eqs. (3), (17), and (18)] from energy-level data.[24–26] The (+) symbols denote *ab initio* MCDF calculations.[25,26]

In computing the mixing angles, the data compilations of Ref. 24 for $Z \le 42$ have been supplemented for $43 \le Z \le 92$ by theoretical energy-level values from the MCDF calculations of Huang[25] for the Si sequence and of Saloman and Kim[26] for the S sequence. The *ab initio* calculations of the line strength are also drawn from the MCDF calculations of Refs. 25 and 26. Because of the labeling convention used in some versions of the MCDF codes, the published compilations do not trace isoelectronic trends past an anticrossing with a level from another strongly interacting configuration. The *LS* labeling is only nominal, with the dominant configuration often differing at the high- and low-Z limits, and some compilations follow the energy ordering rather than the symmetry properties of the levels. Thus two different isoelectronic trends are sometimes joined at an anticrossing.[27] This occurs in the Si sequence[25] for the $^1D_2$ level above $Z=76$, and for the S sequence[26,27] for the $^3P_1$ level above $Z=89$, for the $^1D_2$ level above $Z=80$, and for the $^1S_0$ level above $Z=68$, and accounts for the high-Z termination of some theoretical loci in Figs. 5 and 6.

The agreement between semiempirical and *ab initio* calculations for the Si sequence is good, and becomes nearly exact if the semiempirical results are shifted *upward* by one unit of Z (in contrast to a *downward* shift by one unit of Z observed for the helium sequence). For the

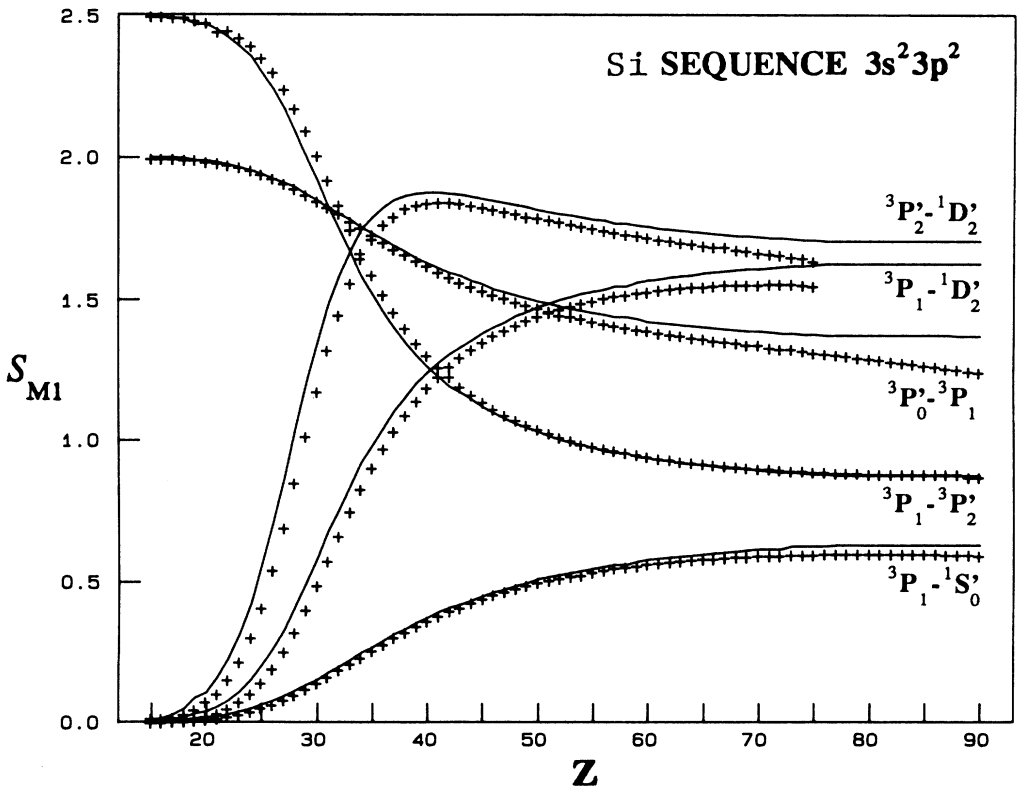

FIG. 5. Line strengths for the $M1$ transitions within the $3s^23p^2$ ground configuration of the Si isoelectronic sequence. The solid lines denote calculations made using Eqs. (30) with empirical mixing angles, and *LS* coupling formulas for the transition moments. The symbols (+) represent the *ab initio* MCDF calculations of Huang (Ref. 25).

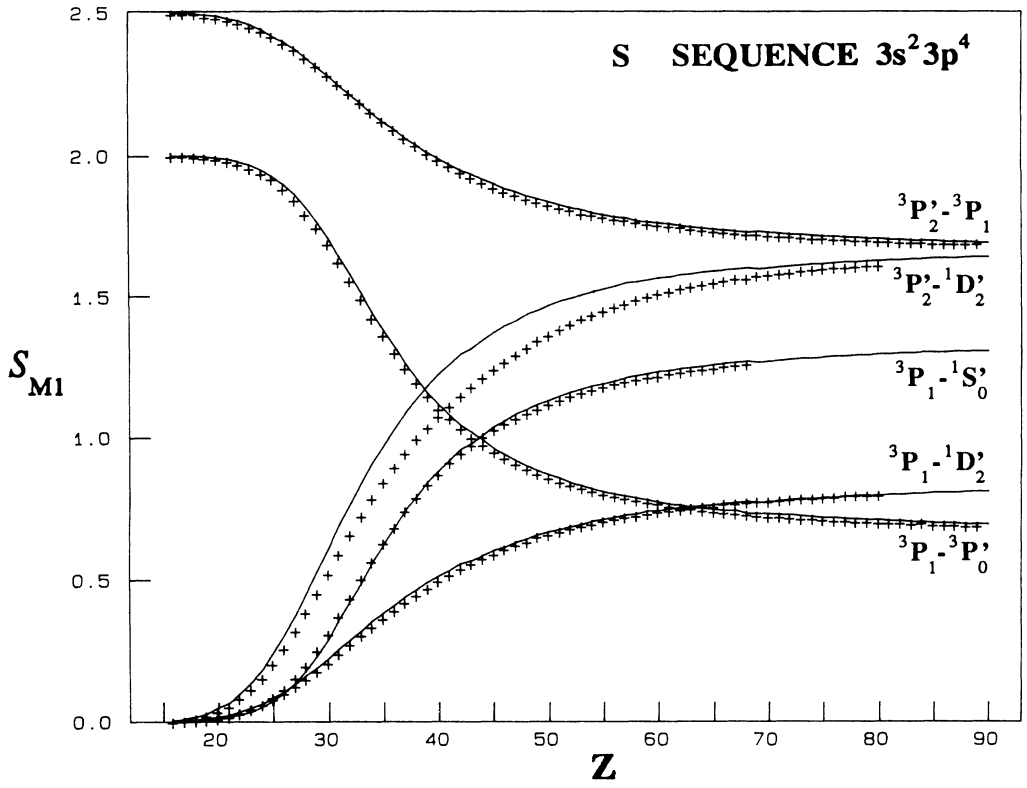

FIG. 6. Line strengths for the $M1$ transitions within the $3s^2 3p^4$ ground configuration of the S isoelectronic sequence. The solid lines denote calculations made using Eqs. (30) with empirical mixing angles and LS coupling formulas for the transition moments. The symbols (+) represent the *ab initio* MCDF calculations of Saloman and Kim (Ref. 26).

S sequence, no shift is indicated, and agreement is good for all transitions except $^3P'_2$-$^1D'_2$. The small discrepancy between semiempirical and *ab initio* values exhibited there may indicate the presence of strong configuration interaction effects.

Radiative branching ratios of $M1$ transitions from the same upper level are sometimes used for calibration purposes. For example, in Ref. 28 the branching ratio for decays from the $3p^2\,{}^1D_2$ level was used for a radiometric calibration of an optical spectrometer. In this case the ratio of intensities is proportional (to within detection efficiency factors) to the ratio of transition probabilities. As seen from Eqs. (20) and (30) this is given by

$$\frac{A(^3P'_2-{}^1D'_2)}{A(^3P'_1-{}^1D'_2)}=\left[\frac{E(^1D'_2)-E(^3P'_2)}{E(^1D'_2)-E(^3P'_1)}\right]^3 3\cos^2(\theta_2)\ , \tag{31}$$

and, by virtue of Eqs. (3) and (18), this ratio is entirely specified (in the single configuration approximation) by measured energy levels.

IV. GYROMAGNETIC RATIOS

The energy of interaction of an atom with an external field **B** can be written as

$$E_{\rm mag}=\mu_0\langle i\|(\mathbf{L}+g_e\mathbf{S})\cdot\mathbf{B}\|k\rangle=\mu_0 g_J M_J\ , \tag{32}$$

where the magnetic moment operator is defined as in Eq. (23), μ_0 is the Bohr magneton, and g_J is the magnetic g factor. In the limit of pure LS coupling and the approximation of the Dirac moment $g_e=2$, the g factor assumes the Landé value (for $J\neq 0$)

$$g_{LSJ}=[3J(J+1)-L(L+1)+S(S+1)]/2J(J+1)\ . \tag{33}$$

If there is intermediate coupling between two levels LSJ and $L'S'J$ as in the case of Eqs. (10) and (19), then the physical g factors can be written[13] in terms of the mixing angles and the Landé g factors as

$$\begin{aligned} g'_{LSJ}&=g_{LSJ}\cos^2(\theta_J)+g_{L'S'J}\sin^2(\theta_J)\ ,\\ g'_{L'S'J}&=g_{LSJ}\sin^2(\theta_J)+g_{L'S'J}\cos^2(\theta_J)\ . \end{aligned} \tag{34}$$

Thus measured energy-level data can be used in conjunction with Eqs. (3) and either Eq. (9) or Eqs. (17) and (18) to determine the mixing angles, and combined with LS values from Eq. (33) to specify physical g values by Eq. (34).

The $4p^5 5s$ configuration in Kr I and the $6s^2 6p^2$ configuration in Pb I

Table III presents two applications of the method: the $4p^2 5s$ configuration in Kr I involves mixing angles com-

puted as described in Sec. II A; the $6s^26p^2$ configuration in Pb I involves mixing angles computed as described in Sec. II B. Mixing angles were obtained from measured energy-level data. For the Kr I case, energy-level data was taken from the measurements of Kaufman and Humphreys.[29] Energy-level data for the Pb I case and g-factor data were taken from Ref. 30. The agreement between the calculated and measured g factors indicates that these systems are dominated by intermediate coupling effects.

These computations provide a clear comparison between configuration interaction and intermediate coupling effects. Deviations of a physical g factor from its (nonzero) Landé value for levels that are *not* mixed by intermediate coupling ($^3P_2$ for sp configurations, $^3P_1$ for p^2 configurations) indicate configuration interaction. Agreement with Eq. (34) for levels with nonzero Landé values that *are* mixed by intermediate coupling ($^3P_1$ and $^1P_1$ for sp configurations; $^3P_2$ and $^1D_2$ for p^2 configurations) indicates intermediate coupling. This method is particularly useful for applications to ionized atomic systems, for which little experimental g factor data presently exist.

TABLE III. Intermediate coupling calculation of g factors for the $4p^55s$ levels in Kr I and the $6s^26p^2$ levels in Pb I.

Level	E (cm^{-1})	Landé[a]	g_J Predict[b]	Expt.[c]
Kr I $4p^55s$, $\sin(\theta_1)=0.717$				
$^3P_2$	79 972[d]	$\frac{3}{2}$	1.500	1.502
$^3P_1$	80 917[d]	$\frac{3}{2}$	1.243	1.242
$^3P_0$	85 192[d]	$\frac{0}{0}$[e]	0/0[e]	
$^1P_1$	85 847[d]	1	1.257	1.259
Pb I $6s^26p^2$, $\sin(\theta_0)=0.377$, $\sin(\theta_2)=0.640$				
$^3P_0$	0	$\frac{0}{0}$[e]	0/0[e]	
$^3P_1$	7 819[c]	$\frac{3}{2}$	1.500	1.501
$^3P_2$	10 650[c]	$\frac{3}{2}$	1.295	1.269
$^1D_2$	21 458[c]	1	1.205	1.230
$^1S_0$	29 467[c]	$\frac{0}{0}$[e]	0/0[e]	

[a]Obtained from Eq. (33).
[b]Obtained from Eq. (34).
[c]Moore, Ref. 30.
[d]Kaufman and Humphreys, Ref. 29.
[e]g_J is undefined for $J=0$.

V. CONCLUSION

It has been shown that intermediate coupling effects in wave functions of $nsn'l$, $nsn'p^5$, np^2, and np^4 configurations can often be reliably parametrized using singlet-triplet mixing angles deduced from energy-level data. The mixing angles can then be used in conjunction with simple LS coupling formulas to reliably predict $M1$ transition probabilities and g factors. The mixing angles can also be used to predict $E1$ transition probabilities if a reasonable approximation to the transition moment can be obtained. In the cases studied here, it was found that good predictions could be made using very simple approximations to the transition moment (hydrogenlike, Coulomb approximation, or scaled values from a neighboring isoelectronic sequence). Although these methods cannot be expected to work well in cases where strong configuration interaction effects are present, these effects often occur locally in an isoelectronic sequence, and can be identified by isoelectronic irregularities in the energy-level data.

Although powerful *ab initio* codes presently exist which permit direct numerical computation of oscillator strengths and g factors for complex systems, this simple mixing angle approach can be provide a useful aid in the prediction, interpretation, and systematization of data. It provides a unique prediction in terms of energy-level data that is independent of methodologies; it incorporates empirical information into the calculation and compares interactions that sample differing portions of the wave function; it provides a means of characterizing and separating intermediate coupling and configuration interaction; it reveals inconsistencies within large blocks of data; and it provides a sensitive way to characterize the agreement between experiment and *ab initio* theoretical predictions.

ACKNOWLEDGMENTS

I am grateful to Dr. Roger Haar, Dr. David Ellis, and Dr. Constantine Theodosiou for valuable suggestions, and to Dr. Gordon Drake and Dr. Jack Sugar for providing me with research results prior to publication. This work was supported by the U.S. Department of Energy, Office of Basic Energy Sciences, Division of Chemical Sciences, under Grant No. DE-FG05-88ER13958.

[1]B. Edlén, in *Spektroskopie I,* Vol. 27 of *Handbuch der Physik,* edited by S. Flügge (Springer, Berlin, 1964), pp. 80–220.
[2]C. E. Theodosiou and L. J. Curtis, Phys. Rev. A **38**, 4435 (1988).
[3]Cf. references given by C. E. Theodosiou, Phys. Rev. A **30**, 2881 (1984).
[4]L. J. Curtis, J. Phys. B **22**, L267 (1989).
[5]E. U. Condon and G. H. Shortley, *The Theory of Atomic Spectra* (Cambridge University Press, Cambridge, 1935).
[6]G. W. F. Drake, Can. J. Phys. **66**, 586 (1988).
[7]L. A. Vainshtein and U. I. Safronova, Phys. Scr. **31**, 519 (1985).
[8]G. W. F. Drake, Nucl. Instrum. Methods **202**, 273 (1982).
[9]G. W. F. Drake, Phys. Rev. A **19**, 1387 (1979).
[10]A. M. Ermolaev and M. Jones, J. Phys. B **7**, 199 (1974).
[11]D. H. Sampson, A. D. Parks, and R. E. H. Clark, Phys. Rev. A **17**, 1619 (1978).
[12]C. D. Lin, W. R. Johnson, and A. Dalgarno, Phys. Rev. A **15**, 154 (1977).

[13]R. D. Cowan, *The Theory of Atomic Structure and Spectra* (University of California Press, Berkeley, 1981).
[14]S. Pasternack, Astrophys. J. **92**, 129 (1940).
[15]G. H. Shortley, Phys. Rev. **57**, 225 (1940).
[16]C. E. Theodosiou, Fortran Program Camatrel, University of Toledo, 1983.
[17]A. Dalgarno and E. M. Parkinson, Proc. R. Soc. London Ser. A **301**, 253 (1967).
[18]J. Sugar, V. Kaufman, P. Indelicato, and W. L. Rowan, J. Opt. Soc. Am. B **6**, 1437 (1989).
[19]K.-T. Cheng and W. R. Johnson, Phys. Rev. A **16**, 263 (1977).
[20]Y.-K. Kim and K.-T. Cheng, J. Opt. Soc. Am. **68**, 836 (1978).
[21]K.-T. Cheng, Y.-K. Kim, and J. P. Desclaux, At. Data Nucl. Data Tables **24**, 111 (1979).
[22]E. P. Ivanova and A. V. Glushkov, J. Quant. Spectrosc. Radiat. Transfer **36**, 127 (1986).
[23]E. Biémont and J. E. Hansen, At. Data Nucl. Data Tables **37**, 1 (1987).
[24]V. Kaufman and J. Sugar, J. Phys. Chem. Rev. Data **15**, 321 (1986).
[25]K.-N. Huang, At. Data Nucl. Data Tables **32**, 503 (1985).
[26]E. B. Saloman and Y.-K. Kim, At. Data Nucl. Data Tables **41**, 339 (1989).
[27]E. B. Saloman and Y.-K. Kim, Phys. Rev. A **38**, 577 (1988).
[28]R. U. Datla, J. R. Roberts, N. Woodward, S. Lippman, and W. L. Rowan, Phys. Rev. A **40**, 1484 (1989).
[29]V. Kaufman and C. J. Humphreys, J. Opt. Soc. Am. **59**, 1614 (1969).
[30]C. E. Moore, *Atomic Energy Levels,* Natl. Bur. Stand. Ref. Data Ser., Natl. Bur. Stand. (U.S.) Circ. No. 35 (U.S. GPO, Washington, D.C., 1958), Vol. 3.